# JOINT ANALOG AND DIGITAL SELF-INTERFERENCE CANCELLATION AND FULL-DUPLEX SYSTEM PERFORMANCE

*Visa Tapio, Hirley Alves, Markku Juntti*

Centre for Wireless Communicatins, University of Oulu, Finland

## ABSTRACT

The challenges with full-duplex transceiver (FD) implementation and transmission in small area radio communication systems are introduced. The main challenge in the FD transceiver design is the self-interference (SI). A three-stage SI cancellation is used for SI mitigation. Analog SI isolation is performed at radio frequency (RF) by utilizing an antenna design based on the characteristic modes theory and using active cancellation principle. Phase and attenuation values of the active cancellation signal path are tuned while transmitting a data signal to a distant node. After the tuning the SI isolation at RF is 90 dB. The remaining SI is then cancelled at baseband. For the baseband SI cancellation an estimate of the SI channel is needed. SI channel estimation is done in full-duplex mode and since the receiver has full knowledge of the transmitted signal no extra pilots are used for the SI cancellation.

***Index Terms***— Full-duplex, self-interference, adaptive cancellation

## 1. INTRODUCTION

FD transceivers can transmit and receive simultaneously at the same carrier frequency offering the potential to double the spectral efficiency, to reduce air interface delays, and to facilitate improved collision detection and avoidance mechanisms in content based networks [1]. Therefore, FD transmission concept is identified as one possible technique for 5G systems [2], [3]. Other benefits as well as challenges in FD systems development have been reviewed in, e.g., [4], [5], [6], [7]. Despite these fundamental results and achievements, there are still many challenges and open problems to resolve, ranging from FD transceiver design to the network level operation. For instance, a FD transceiver is capable to handling simultaneous uplink and downlink traffic [8]. Nonetheless, in the network level there will be an increase in the intra and inter-cell interference, which may hamper the performance of the FD devices. To this end, the authors in [9], [10], [11] shed some light into these issues by assessing the spectral efficiency, the outage probability and throughput in a network level deployment of FD nodes. Another potential application is in relaying networks, where the relay operates in a FD fashion while other nodes are half-duplex (HD), which eliminates the inherent issue of multiplexing loss of HD relaying [4], [12], [13].

The main problem in the FD transceiver design is the SI, i.e., the leakage of the transmit signal to the device's own receiver. Depending on the system, the SI cancellation requirement can be well over 100 dB. In order to achieve such a high isolation levels, the SI cancellation must be done at different stages. Reviews on different SI cancellation techniques can be found, e.g., in [3], [14], [15]. In this paper, the analog cancellation is done at RF using an active cancellation principle, where a feed-forward path consisting of a phase shifter and attenuator is added in parallel to the transmit and receive antenna ports. Since the attenuation and phase settings of the active cancellation can change during the operation, they must be tunable. The usage of a gradient descent algorithm for the tuning has been proposed in [16]. The tuning of the active cancellation circuitry is done in HD mode using the transmitted data signal without the need to use a specific tuning signal, i.e., the data transmission can be continuous.

The remaining SI after the first cancellation stage is cancelled at the baseband. Therein the SI channel is first estimated. The SI channel estimate and the known transmitted signal are then used to form a signal that is subtracted from the received signal. The SI channel estimation is performed during the reception of the signal from a distant node using the transmitted data signal. Hence, neither additional pilot symbols nor silent periods are needed for the SI channel estimation [17].

The rest of the paper is organized as follows. The transceiver model and SI cancellation is described in Section 2 and numerical results are presented in Section 3. Finally, conclusions are presented in Section 4.

## 2. TRANSCEIVER AND SELF-INTERFERENCE CANCELLATION

The self-interference cancellation is performed with three techniques: antenna isolation, active cancellation at RF and digital cancellation. The antenna design is based on the characteristic modes theory [18], [19]. The antenna offers 61 dB

This work has been partially funded by the Academy of Finland and by Tekes - the Finnish Funding Agency for Innovation, Nokia Oyj, Esju Oy and CoreHW Oy.

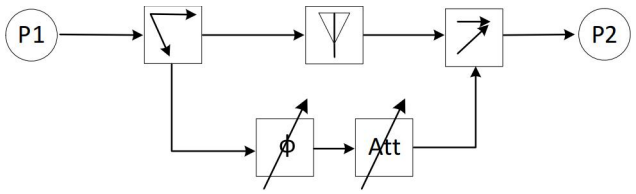


**Fig. 1**. Antenna and active cancellation.

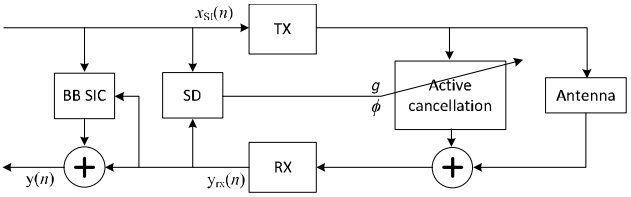


**Fig. 2**. Tuning of the active cancellation and baseband SI cancellation.

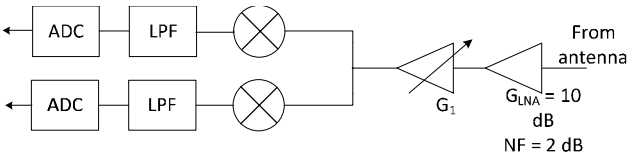


**Fig. 3**. Direct conversion receiver.

isolation over 20 MHz bandwidth. For the RF cancellation, an additional signal path consisting of a phase shifter ($\phi$) and attenuator (Att) is added in parallel to the antenna to provide additional isolation, see Fig. 1. Port P1 is the transmitter's antenna port and P2 is the receiver's antenna port. Power splitter after P1 is used to sample the transmitted signal for analog SI isolation. The signal power fed to the phase shifter is 20 dB lower than that at port P1 and 99% of the power is propagating to the antenna. The power splitter can be implemented as a 20 dB directional coupler. The power combiner before P2 is used to sum up the SI signal and the output signal of the attenuator. The signal from the attenuator is further attenuated by 20 dB in the power combiner and it can be also be implemented as a directional coupler.

Since the SI path from the transmitter to the receiver can change during the operation the phase and attenuation of the SI isolation path must be tunable. The tuning of the SI isolation path is done using the transmitted data signal, i.e., no extra pilot symbols are needed for the baseband SI cancellation. The principle of the tuning is shown in Fig. 2. The steepest descent (SD) adaptive algorithm used for the tuning of the attenuation ($g$) and phase ($\phi$) is

$$\begin{aligned} w(k+1) &= w(k) - \frac{\beta}{M\sqrt{P_{\mathrm{x}}P_{rx}}}\sum_{n=1}^{M} y_{\mathrm{rx}}(n)x_{\mathrm{SI}}^{*}(n) \\ g(k+1) &= Q\{10\cdot\log_{10}|w(k+1)|\} \\ \phi(k+1) &= Q\{\arctan\frac{\Im(w(k+1))}{\Re(w(k+1)}\}, \end{aligned} \tag{1}$$

where $k$ is iteration index, $M$ is the number of samples per iteration, $P_{\mathrm{x}}$ is the power of the SI signal $x_{\mathrm{SI}}$ at baseband, $P_{\mathrm{rx}}$ is the power of the input signal $y_{\mathrm{rx}}$ at baseband, $\beta$ is step size, and $Q\{\cdot\}$ is quantization operation. The phase and gain values are quantized since attenuators and phase shifters are typically controlled in fixed steps. The values of the attenuator and phase shifter at the beginning of the tuning process are initialized as $g(1)$ and $\phi(1)$, respectively and $w(1)$ is

$$w(1) = |10^{g(1)/10}|\cdot e^{j\phi(1)}. \tag{2}$$

After each iteration the absolute value of the cross correlation $c(m)$ between the transmitted SI signal and the received signal is calculated as [20]

$$\begin{aligned} c(n) &= R_{xy}(n-N), \text{where} \\ R_{xy}(n) &= \sum_{i=0}^{N-n-1} x_{\mathrm{SI}}(i+n)y_{\mathrm{rx}}^{*}(i). \end{aligned} \tag{3}$$

If the peak value of the cross-correlation at iteration $k$ is smaller than that at iteration $k-1$ the tuning is continued. If the peak value is the same or larger than at the previous iteration the tuning is stopped and phase and attenuation values from the iteration $k-1$ are selected to be used in the active cancellation.

The RX block in Fig. 2 is a direct conversion receiver with 12-bit analog-to-digital (AD) converters (Fig. 3). The low noise amplifier gain and noise figure used in simulations are 10 dB and 2 dB, respectively. The variable gain amplifier (G1) is used to scale the signal power before the AD conversion.

The residual SI after the RF cancellation is further reduced with baseband processing as shown in Fig. 2. The SI channel is estimated using minimum mean square error (MMSE) estimator

$$\hat{\mathbf{h}}_{\mathrm{SI}} = \mathbf{R}_x^{-1}\mathbf{r}, \tag{4}$$

where $\mathbf{R}_x$ is the autocorrelation matrix of the transmitted self-interference ($\mathbf{x}_{SI}$) and $\mathbf{r}$ is the vector of cross-correlations between the received signal after the SI cancellation $y(n)$ and $x_{SI}(n)$.

The SI channel estimate is used to form a replica of the remaining SI signal, which is then subtracted from the received baseband signal. The signal after the baseband SI cancellation is then

$$\mathbf{y} = \mathbf{y}_{\mathrm{d}} + \mathbf{X}_{\mathrm{SI}}(\mathbf{h}_{\mathrm{SI}} - \hat{\mathbf{h}}_{\mathrm{SI}}) + \mathbf{w}. \tag{5}$$

After the SI cancellation, synchronization, channel estimation and data detection are performed for the desired signal. Channel for the desired signal is estimated utilizing the long training sequence (LTS) of the IEEE 802.11 [21]. The channel estimate at sub-carrier $k$ is [22]

$$h_k = \frac{1}{2}(y_{1,k} + y_{2,k})x_k^*, \tag{6}$$

where $y_{i,k}$ is the received sample at sub-carrier $k$ during the reception of the $i^{\text{th}}$ symbol of the LTS, $x_k$ is the $k^{\text{th}}$ element of the LTS symbol. Two identical LTS symbols are sent during the beginning of a frame.

## 3. NUMERICAL RESULTS

The signal used in simulations is an orthogonal frequency-division multiplexing (OFDM) signal with 48 data sub-carriers and 4 pilot sub-carriers at 3.5 GHz center frequency. Data sub-carriers are modulated using 16 level quadrature amplitude modulation (16-QAM). The bandwidth of the signal is 20 MHz. The antenna is modelled using an electromagnetic simulation tool (CST Microwave Studio). Simulated S-parameters are brought to the system model as a S-parameter file. The FD transceiver including the analog SI isolation is modelled using the Advanced Design System (ADS). Baseband signal generation and the baseband FD receiver including the control of the SI isolation are implemented using Matlab. The starting point for the Matlab model development has been the OFDM simulation model from [23]. Baseband and RF models are included in the same simulation model allowing to model the interplay between the RF and baseband domains.

Examples of the tuning performance are is shown in Fig. 4. The initial values of the attenuator and phase shifter are $-15$ dB and 0 degree, respectively, and the gain of the amplifier G1 in Fig. 3 is set to 0 dB to prevent overloading of the AD converters. In one iteration, 100 OFDM symbols

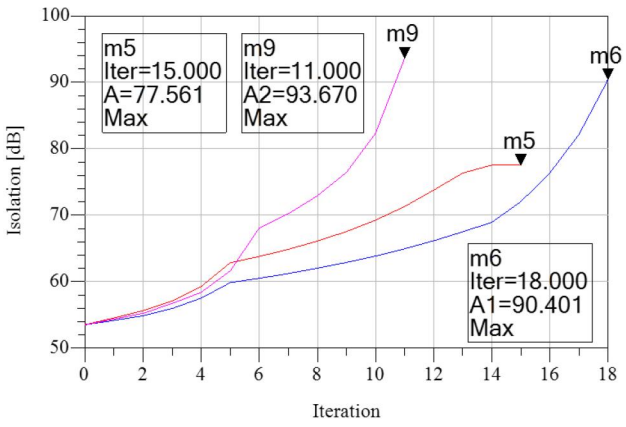


**Fig. 4**. Tuning of analog SI cancellation.

**Table 1**. SI cancellation (SIC) values.

| | 0.25 dB | | 0.5 dB | | 1.0 dB | |
|---|---|---|---|---|---|---|
| Ph | SIC | Iter. | SIC | Iter. | SIC | Iter. |
| 0° | 94 | 11 | 90 | 18 | 78 | 15 |
| 90° | 90 | 15 | 90 | 22 | 90 | 19 |
| 180° | 90 | 9 | 90 | 14 | 78 | 10 |
| 270° | 89 | 5 | 90 | 5 | 78 | 4 |

including cyclic prefixes are sent. With the used signal model this corresponds to 0.4 ms per iteration. If the phase and and attenuation of the feed-forward path are far from the optimal values and the step size is too small, the convergence of the SD algorithm is slow and in some cases the cross-correlation based criterion can stop the algorithm too early. To prevent this, a variable step size is used. In the first five iterations, the step size $\beta$ in the steepest descent algorithm (1) has been $5 \cdot 10^{-3}$ and after this the step size decreases to $1 \cdot 10^{-3}$. The red curve with the marker m5 shows the performance when the phase and attenuation tuning resolution are 5 degrees and 1.0 dB, respectively. The blue curve (m6) shows the performance when the attenuation resolution is decreased to 0.5 dB. The magenta curve (m9) shows the performance when the attenuation resolution is further decreased to 0.25 dB and in the six first iterations $\beta$ is $5 \cdot 10^{-3}$ before switching to $1 \cdot 10^{-3}$. The SI cancellation performance with different initial phase values of 0°, 90°, 180° and 270° are shown in Table 1. With 1 dB attenuation resolution the SI cancellation performance changes from 78 to 90 dB. With further simulations it was found out that when the initial phase value is between 26° and 139° or between 281° and 307° the SI cancellation at RF after tuning is 90 dB and when the initial value is not inside these regions the SI cancellation is 78 dB. This variation of SI cancellation performance indicates that the 1 dB resolution is too low for the tuning. With 0.25 dB and 0.5 dB resolution the SI isolation is 90 dB or more regardless of the initial phase settings of the feed-forward path.

Bit-error-rate (BER) performance of an un-coded FD link was also evaluated. In BER simulations the initial phase and attenuation values of the analog SI have been 180° and $-15$ dB and the phase and attenuation resolution in the tuning phase have been 5° and 0.5 dB, respectively. After the tuning has stopped the system switches to FD mode and the gain of the amplifier G1 is set to 35 dB. BER results as a function of the bit energy to noise spectral density ratio ($E_b/N_0$) are shown in Fig. 5. $E_b/N_0$ values correspond to received signal powers from $-90$ dBm to $-70$ dBm. The blue curve with asterisks shows the BER of the FD link when, 60 OFDM symbols are used for the SI channel estimation and the channel between the nodes has been an additive white Gaussian noise channel (AWGN). The magenta curve with triangles shows the performance when 100 OFDM symbols are used for the SI channel estimation. The red curve with circles shows the BER of a HD link and the dashed black curve

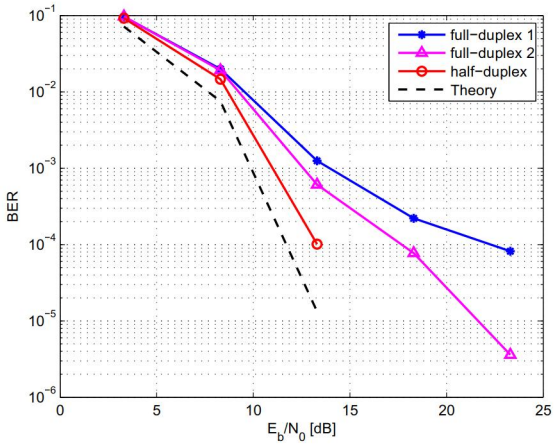


**Fig. 5**. BER results.

shows the theoretical BER of HD 16-QAM modulation in an AWGN channel calculated with Matlab's `berawgn` function [20]. The difference between the BER of the HD link and theoretical curve is due to the channel estimation in (6). Since the SI channel estimation is done during the data reception from a distant node, the desired signal acts as a interference for the SI channel estimation. Its effect can be mitigated by increasing the number of signal samples in SI estimation as seen from full-duplex 1 and full-duplex 2 curvers in Fig. 5.

## 4. CONCLUSIONS

A three-step SI cancellation was considered. Antenna design based on the characteristic modes theory provides 61 dB isolation. The isolation at RF is further increased by utilizing a feed-forward path from the transmitter's power amplifier output to the receiver's low-noise amplifier input. The attenuation and phase shift of the feed-forward path must be accurately tuned in order to gain this additional SI isolation. The tuning is performed in a HD mode using the transmitted signal and the variable step steepest descent algorithm. After the tuning up to 33 dB additional isolation is gained resulting in total RF isolation of 94 dB. After the tuning of the feed-forward path is accomplished the system switches to FD mode. The residual self-interference is cancelled by estimating the SI channel using the transmitted data signal. The estimated SI channel is then used to form a estimate of the residual SI which is then subtracted from the received signal. After the synchronization, channel estimation an data detection of the desired signal the BER is used to measure the FD link performance in an AWGN channel.

### 4.1. Potential Applications and Future Work

As aforementioned FD communications can enhance the spectral efficiency of wireless networks and thus is a potential candidate for 5G. Besides, FD transceivers can support simultaneous uplink and downlink traffic, which can be also used for in-band wireless backhaul applications as pointed out in [4]. Furthermore, another promising application for FD transceivers is in relaying networks, which is closer to a practical scenario, since terminal nodes would be HD, while the base station is FD as evinced in [1] as well as in [12].

As a future work, we intend to consider fading channels and extend the proposed design. First, we aim to analytically model the received signal as a function of the transceiver impairments imposed at the RF chain (e.g. power amplifier nonlinearities, phase noise, quantization), thus quantifying its effect into signal of interest. Some models already exist [24], but do no focus on FD transceivers nor the multiplicative effect of the imperfections on the system performance. This model allows us to better characterize the performance of the FD transceiver in more practical scenarios such as FD relaying and self-backhauling.

## ACKNOWLEDGMENT

Antenna s-parameter files were provided by Dr. Marko Sonkki, University of Oulu/Centre for Wireless Communications.

## 5. REFERENCES

[1] K. Rikkinen, V. Tapio, H. Alves, M. Al-Imari, A. C. Cirik, J. Seddar, A. Sethi, B. Debaillie, and C. Lavin, "Full-duplex transmission in small area radio communication systems," in *2015 IEEE 20th International Workshop onComputer Aided Modelling and Design of Communication Links and Networks (CAMAD)*, Sept 2015, pp. 1–5.

[2] "NGMN 5G white paper," Tech. Rep., Next Generation Mobile Networks (NGMN) Alliance, February 2015.

[3] Z. Zhang, X. Chai, K. Long, A. V. Vasilakos, and L. Hanzo, "Full duplex techniques for 5g networks: self-interference cancellation, protocol design, and relay selection," *IEEE Communications Magazine*, vol. 53, no. 5, pp. 128–137, May 2015.

[4] G. Liu, F. R. Yu, H. Ji, V. C. M. Leung, and X. Li, "In-band full-duplex relaying: A survey, research issues and challenges," *IEEE Communications Surveys Tutorials*, vol. 17, no. 2, pp. 500–524, Secondquarter 2015.

[5] S. Hong, J. Brand, J. I. Choi, M. Jain, J. Mehlman, S. Katti, and P. Levis, "Applications of self-interference cancellation in 5g and beyond," *IEEE Communications Magazine*, vol. 52, no. 2, pp. 114–121, February 2014.

[6] D. Kim, H. Lee, and D. Hong, "A survey of in-band full-duplex transmission: From the perspective of phy and

mac layers," *IEEE Communications Surveys Tutorials*, vol. 17, no. 4, pp. 2017–2046, Fourthquarter 2015.

[7] A. Sabharwal, P. Schniter, D. Guo, D. W. Bliss, S. Rangarajan, and R. Wichman, "In-band full-duplex wireless: Challenges and opportunities," *IEEE Journal on Selected Areas in Communications*, vol. 32, no. 9, pp. 1637–1652, Sept 2014.

[8] R. A. Pitaval, O. Tirkkonen, R. Wichman, K. Pajukoski, E. Lahetkangas, and E. Tiirola, "Full-duplex self-backhauling for small-cell 5g networks," *IEEE Wireless Communications*, vol. 22, no. 5, pp. 83–89, October 2015.

[9] C. H. M. de Lima, P. H. J. Nardelli, H. Alves, and M. Latva-aho, "Full-duplex communications in interference networks under composite fading channel," in *2014 European Conference on Networks and Communications (EuCNC)*, June 2014, pp. 1–5.

[10] H. Alves, C. H. M. de Lima, P. H. J. Nardelli, R. Demo Souza, and M. Latva-aho, "On the average spectral efficiency of interference-limited full-duplex networks," in *2014 9th International Conference on Cognitive Radio Oriented Wireless Networks and Communications (CROWNCOM)*, June 2014, pp. 550–554.

[11] Z. Tong and M. Haenggi, "Throughput analysis for full-duplex wireless networks with imperfect self-interference cancellation," *IEEE Transactions on Communications*, vol. 63, no. 11, pp. 4490–4500, Nov 2015.

[12] H. Alves, R. D. Souza, and M. E. Pellenz, "Brief survey on full-duplex relaying and its applications on 5g," in *2015 IEEE 20th International Workshop on Computer Aided Modelling and Design of Communication Links and Networks (CAMAD)*, Sept 2015, pp. 17–21.

[13] H. Q. Ngo, H. A. Suraweera, M. Matthaiou, and E. G. Larsson, "Multipair full-duplex relaying with massive arrays and linear processing," *IEEE Journal on Selected Areas in Communications*, vol. 32, no. 9, pp. 1721–1737, Sept 2014.

[14] M. Heino, D. Korpi, T. Huusari, E. Antonio-Rodriguez, S. Venkatasubramanian, T. Riihonen, L. Anttila, C. Icheln, K. Haneda, R. Wichman, and M. Valkama, "Recent advances in antenna design and interference cancellation algorithms for in-band full duplex relays," *IEEE Communications Magazine*, vol. 53, no. 5, pp. 91–101, May 2015.

[15] B. Debaillie, D. J. van den Broek, C. Lavn, B. van Liempd, E. A. M. Klumperink, C. Palacios, J. Craninckx, B. Nauta, and A. Prssinen, "Analog/rf solutions enabling compact full-duplex radios," *IEEE Journal on Selected Areas in Communications*, vol. 32, no. 9, pp. 1662–1673, Sept 2014.

[16] M. Jain and et al., "Practical, real-time, full duplex wireless," in *Proceedings of the 17th Annual International Conference on Mobile Computing and Networking (MobiCom '11)*, New York, NY, USA, 2011, pp. 301–312, ACM.

[17] V. Tapio and M. Sonkki, "Analog and digital self-interference cancellation for full-duplex transceivers," in *22th European Wireless Conference European Wireless 2016*, May 2016, pp. 1–5.

[18] R. Garbacz and R. Turpin, "A generalized expansion for radiated and scattered fields," *IEEE Transactions on Antennas and Propagation*, vol. 19, no. 3, pp. 348–358, May 1971.

[19] R. Harrington and J. Mautz, "Theory of characteristic modes for conducting bodies," *IEEE Transactions on Antennas and Propagation*, vol. 19, no. 5, pp. 622–628, Sep 1971.

[20] "Matlab documentation," Manual, The MathWorks, Inc.

[21] IEEE Computer Society, "Part 11: Wireless LAN Medium Access Control (MAC) and Physical Layer (PHY) Specifications," Standard, IEEE, 2012.

[22] J. Heiskala and J. Terry, *OFDM Wireless LANs: A Theoretical and Practical Guide* , Sams Publishing.

[23] Rice University WARP project, http://warp.rice.edu.

[24] E. Bjornson, M. Matthaiou, and M. Debbah, "A new look at dual-hop relaying: Performance limits with hardware impairments," *IEEE Transactions on Communications*, vol. 61, no. 11, pp. 4512–4525, November 2013.